

ide/acid ratios go from $\sim 1/11$ in 6% (w/v) solution to $\sim 1/2$ in 30% (w/v) solution. Even as the amide/acid ratio approaches 1/1, only small changes in the ^{15}N shift data are expected since HFIP cannot form a complex like the amide/TFA system. The decrease in the HFIP concentration does cause a small increase in shielding of the ^{15}N nuclei. Studies of higher concentrations could not be done due to insolubility of higher concentrations of the nylon in HFIP.

At the lower nylon concentrations (<25% (w/v) in TFA), the degree of polymerization of nylon 66 (high amine content vs. standard) had little effect on the ^{15}N or ^{13}C chemical shifts. The ^{15}N signal of 35% standard nylon 66 solution is further upfield, however, than the ^{15}N signal of 45% high amine solution (45% standard solution gave no ^{15}N signal). This result is not accounted for by considering the neutralization of TFA by the basic amine end groups (amine/amide ratio is 1/16 for high amine sample and 1/66 for standard sample). The resulting amide/TFA ratios are calculated to be $\sim 1/3$ in the 45% high amine solution and $\sim 1/4$ in the 35% standard solution. The larger upfield shift of the ^{15}N signal in the latter would imply that formation of the amide/TFA complex is enhanced in the higher molecular weight sample. Further experiments to define the influence of degree of polymerization on complex formation are indicated.

The ^1H chemical shift data showed the least sensitivity to changes in concentration and degree of polymerization. The largest changes in the ^1H data were for the proton active in the protonation and/or hydrogen bonding. In TFA, $\Delta\delta_{\text{H}}$ of the acidic proton over the concentration range (6-45%) was 2.6 ppm and in HFIP it was 1.2 ppm. The ^1H NMR spectrum for the 45% standard in TFA, however, showed extreme broadening, in support of fast proton exchange over the NH region (the 35% standard showed less broadening in the same region). In the 45% high amine sample in TFA solution, the NH signal was still present but was dominated by a peak at 7.1 ppm, which may be attributed to hydrogen bonding at the carbonyl oxygen. Thus, looking at the proton spectra, we can quickly determine if the cross-polarization techniques can be used in doing ^{15}N NMR spectroscopy.

Conclusions

The ^{15}N chemical shifts for nylon 66 in trifluoroacetic acid and hexafluoro-2-propanol solutions are more sensitive to changes in polymer concentration than corresponding ^{13}C data. The ^{15}N data exhibit deshielding with decreasing polymer concentration and with increasing solvent acidity. The site of hydrogen bonding and/or protonation in excess acid is the oxygen of the amide carbonyl as shown by the deshielding in the ^{15}N and ^{13}C data of the amide group. In the presence of excess acid, the degree of polymerization of nylon 66 has little effect on ^{15}N chemical shifts, while at higher nylon concentrations, there is an apparent change in the nature of the hydrogen bonding and/or protonation. As the amide/acid ratio approaches 1/1, there is an increase in the rate of proton exchange at the NH proton. This results from a possible complex formation between amide and TFA and/or a conformational change.

Utilization of the adiabatic J cross-polarization (AJCP) technique has provided major signal enhancements and time savings, has eliminated the need to exactly match the radio-frequency amplitudes of the two nuclei during polarization transfer, and, thus, has increased the practicality of ^{15}N NMR. The advantages of using ^{15}N NMR in conjunction with ^1H and ^{13}C NMR data in the elucidation of solute-solvent interactions are great, especially when the ^{15}N data are more responsive than the corresponding ^1H and ^{13}C data as they proved to be for the polyamide systems studied.

References and Notes

- (1) Holmes, B. S.; Chingas, G. C.; Moniz, W. B.; Ferguson, R. C. *Macromolecules* 1981, 14, 1785.
- (2) Schilling, G. S.; Kricheldorf, H. R. *Makromol. Chem.* 1975, 176, 3341.
- (3) McClelland, R. A.; Reynolds, W. F. *J. Chem. Soc., Chem. Commun.* 1974, 824.
- (4) Kricheldorf, H. R.; Hull, W. E. *J. Polym. Sci., Polym. Chem. Ed.* 1978, 16, 583.
- (5) Bertrand, R. D.; Moniz, W. B.; Garroway, A. N.; Chingas, G. C. *J. Am. Chem. Soc.* 1978, 100, 5227. *J. Magn. Reson.* 1978, 32, 465.
- (6) Chingas, G. C.; Garroway, A. N.; Moniz, W. B.; Bertrand, R. D. *J. Am. Chem. Soc.* 1980, 102, 2526.
- (7) Stewart, W. E.; Mandelkern, L.; Glick, R. E. *Biochemistry* 1967, 6, 150.

Small-Angle Neutron Scattering on Bulk Polystyrene with Mismatched M_w [†]

Celia Tangari,[‡] John S. King,* and George C. Summerfield

Department of Nuclear Engineering, The University of Michigan, Ann Arbor, Michigan 48109. Received August 5, 1981

ABSTRACT: Small-angle neutron scattering data have been obtained from a number of bulk polystyrene samples containing high concentrations of deuterated molecules. An equation was earlier derived for the SANS scattering cross section for bulk samples in which the deuterated and protonated molecules have modest differences in physical properties. The limits of validity of the equation are examined here by deliberate mismatch of molecular weights for PSD and PSH. The equation is found to fit the data for a mismatch ratio of molecular weights ($M_w(\text{PSD})/M_w(\text{PSH})$) between 0.32 and 1.94 but does not apply for ratios greater than 2.0.

Introduction

It has been demonstrated¹⁻⁴ that high-concentration marked (deuterated) samples can be used to measure the

single-chain structure factor, with consequent high experimental intensities. The technique requires that the two polymer species be identical except for their neutron scattering lengths. It is difficult, even under ideal experimental conditions, to produce samples in which the two species are identical. They may differ in melting temperatures, in θ temperatures, and particularly in degree of polymerization (molecular weight).

[†] Work supported in part by National Science Foundation Grant No. DMR-79-26254.

[‡] Sponsored by Comissao Nacional de Energia Nuclear/Brazil.

Table I
Sample Characteristics(1) Samples with Matched M_w

sample	$M_w(\text{PSD})$	M_w/M_n	$M_w(\text{PSH})$	M_w/M_n	x	$x(1-x)$
HPSH3D7	194 000	1.15	198 000	1.06	0.684	0.216
HPSH7D3	194 000		198 000		0.285	0.204
MPSH3D7	87 000	1.08	100 000	<1.06	0.700	0.210
MPSH7D3	87 000		100 000		0.300	0.210
LPSH3D7	64 000	1.05	53 700	1.06	0.684	0.216
LPSH7D3	64 000		53 700		0.285	0.204
HPSH95D5	194 000		198 000		0.050	0.0048

(2) Samples with Mismatched M_w

sample	$M_w(\text{PSD})$	M_w/M_n	$M_w(\text{PSH})$	M_w/M_n	$M_w(\text{PSD})/M_w(\text{PSH})$	x	$x(1-x)$
PSMH3HD7	194 000	1.15	100 000	<1.06	1.94	0.7	0.210
PSMH7HD3	194 000		100 000		1.94	0.3	0.210
PSLH3HD7	194 000		53 700	1.06	3.60	0.7	0.210
PSLH5HD5	194 000		53 700		3.60	0.5	0.250
PSLH7HD3	194 000		53 700		3.60	0.3	0.210
PSVLHHD7	194 000		19 800	<1.06	9.80	0.7	0.210
PSVLHHD3	194 000		19 800		9.80	0.3	0.210
PSVLHHD5	194 000		19 800		9.80	0.05	0.0048
PSHH3LD7	64 000	1.05	198 000	1.06	0.32	0.7	0.210
PSHH7LD3	64 000		198 000		0.32	0.3	0.210

In this paper we report SANS data from samples with ratios of molecular weights of deuterated (PSD) to normal (PSH) molecules that vary from 0.32 to 9.8. The data are analyzed with an expression for the cross section that can only be valid for modest ratios. The purpose is to determine the limit of validity when applied to the common problem of matching the marked and host molecules.

Consider a bulk mixture of N_H normal molecules, each having n_H monomers, and N_D deuterated molecules, each having n_D monomers. When the molecular weights are not closely matched, the elastic coherent differential cross section can be written⁵

$$S(Q) = (a_H - a_D)^2 c_p x(1-x) \times [x S_s^H(Q) + (1-x) S_s^D(Q)] + [a_H(1-x) + a_D x]^2 S_T(Q) \quad (1)$$

where a_H and a_D are the scattering lengths per protonated and deuterated monomer, respectively, $c_p = (N_D n_D + N_H n_H)$ is the total number of monomers in the sample, and $x = N_D n_D / c_p$, the fraction of monomers that are deuterated. The three scattering functions of eq 1 are

$$S_s^H(Q) = \frac{1}{N_H n_H} \sum_{N,j,j'} e^{i\mathbf{Q} \cdot (\mathbf{r}_j - \mathbf{r}_{j'})}; \quad S_s^H(0) = n_H \quad (2a)$$

$$S_s^D(Q) = \frac{1}{N_D n_D} \sum_{M,l,l'} e^{i\mathbf{Q} \cdot (\mathbf{r}_l - \mathbf{r}_{l'})}; \quad S_s^D(0) = n_D \quad (2b)$$

$$S_T(Q) = \sum_{N,j,j'} e^{i\mathbf{Q} \cdot (\mathbf{r}_j - \mathbf{r}_{j'})} + \sum_{M,l,l'} e^{i\mathbf{Q} \cdot (\mathbf{r}_l - \mathbf{r}_{l'})} + \sum_{N \neq M} \sum_{j,j'} e^{i\mathbf{Q} \cdot (\mathbf{R}_N - \mathbf{R}_M + \mathbf{r}_j - \mathbf{r}_{j'})} + \sum_{M \neq N} \sum_{l,l'} e^{i\mathbf{Q} \cdot (\mathbf{R}_M - \mathbf{R}_N + \mathbf{r}_l - \mathbf{r}_{l'})} + 2 \text{Re} \sum_{N,M} \sum_{j,l} e^{i\mathbf{Q} \cdot (\mathbf{R}_N - \mathbf{R}_M + \mathbf{r}_j - \mathbf{r}_l)} \quad (2c)$$

where \mathbf{R}_N is the center of mass position of the N th protonated chain and \mathbf{r}_j the position of the j th monomer of the N th chain relative to \mathbf{R}_N . The quantities \mathbf{R}_M and \mathbf{r}_l are similarly defined for the deuterated chains. If the two species are identical, then

$$S_s^D(Q) = S_s^H(Q) = S_s(Q)$$

and the usual result is obtained:

$$S(Q) = (a_H - a_D)^2 c_p x(1-x) S_s(Q) + [a_H(1-x) + a_D x]^2 S_T(Q) \quad (3)$$

The function $S_T(Q)$ defined in eq 2c is the contribution from density fluctuations; it is the cross section one would obtain if every monomer scattered with the same amplitude, $a_H(1-x) + a_D x$. It should therefore be proportional to the cross section, $S_X(Q)$, from a small-angle X-ray measurement. It is possible to use $S_X(Q)$ to eliminate $S_T(Q)$ from eq 1. Here, however, we will assume that $S_T(Q)$ is independent of x and can be measured by neutron scattering from a blank sample for which $x = 1$.

To extract $S_s^H(Q)$ and $S_s^D(Q)$, measurements are made on two samples with different deuterated fractions, for example, x_1 and x_2 . After eliminating $S_T(Q)$ from eq 1, for each case, we solve the equations to obtain $S_s^H(Q)$ and $S_s^D(Q)$.

Experimental Procedure

Several bulk mixtures of polystyrene were prepared with different molecular weights and deuterated fractions. These were prepared by freeze-drying particles from benzene solutions and vacuum molding at 120 °C and approximately 750 psi. The samples were then cooled at a rate of 1.3 °C/min in the first hour, after which a temperature below the glass transition temperature was reached. The cooling rate then dropped to 0.6 °C/min. The samples with PSH of very low molecular weight (19 800) were cooled very slowly (0.2 °C/min) through the glass transition temperature. Clear wafers 2.0 cm in diameter were obtained. The thicknesses varied from 0.07 to 0.12 cm. Table I gives the characteristics of the polymer materials used as reported by several sources.⁶ The samples are divided into two groups according to the way in which the data were analyzed, using eq 1 for mismatched samples and eq 3 for matched samples.

The experiments were performed at the University of Missouri research reactor SANS spectrometer. The beam geometry is given in Table II. A detailed description of the spectrometer can be found in ref 7. Figure 1 is a plot of the observed intensities, corrected to unit transmission, for open sample holder, 100% PSD and 100% PSH blanks, and a 5% deuterated sample. The actual intensities, in the absence of the semitransparent gadolinium beam stop, require raising the four points below $Q = 0.006 \text{ \AA}^{-1}$ by a factor of 200. The detector efficiency vs. Q is nearly flat. A small falloff at large Q is observed from incoherent scattering, requiring corrections of 2.2% at $Q = 0.037 \text{ \AA}^{-1}$ and 4.8% at $Q = 0.079 \text{ \AA}^{-1}$. A small oscillation is seen at low Q , whose period coincides with the alternating two-layer detector separation. This apparently introduces an additive constant oscillation to all scattering profiles, but this is negligibly small for our samples and is, in principle, removed by the open-beam background subtraction.

Table II
Beam Geometry of the MURR Spectrometer

λ	4.75 Å
$\Delta\lambda/\lambda$	4.1%
ΔQ	0.005 Å ⁻¹ , nearly independent of Q
D^a	4.5 m
d^b	4.5 m
Q range	0.00675–0.08 Å ⁻¹ ^c
source iris	2.0-cm diam
sample iris	1.0-cm diam

^a D = source-sample distance. ^b d = sample-detector distance. ^c A semitransparent gadolinium beam stop extends to $Q = 0.006$ Å⁻¹.

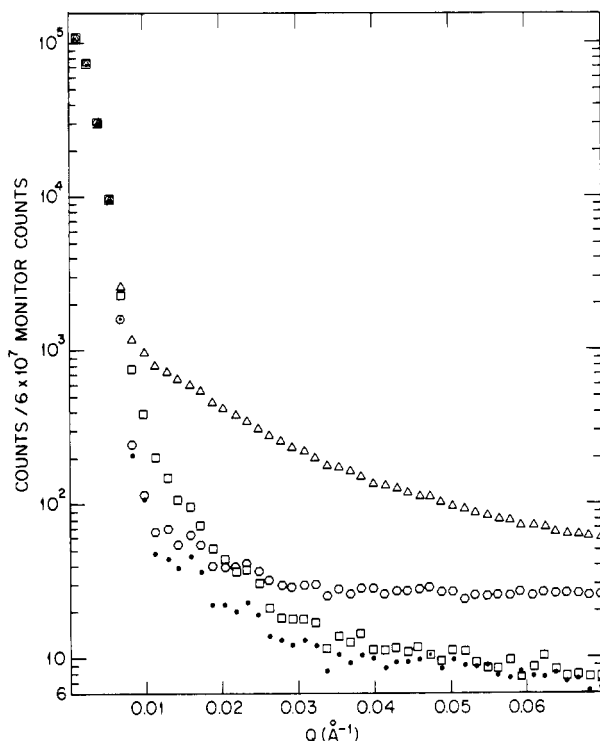


Figure 1. Transmission-corrected intensities for the MURR-SANS spectrometer. Data points correspond to open beam (●), 100% PSD (□), 100% PSH (○), and the 5% PSD/95% PSH sample HPSH95D5 (Δ).

The measured intensities of all samples and the open beam are corrected for beam-blocked background. All samples are then normalized to unit transmission and constant thickness and finally the corrected open-beam intensity is subtracted. The single-chain intensity $I_{sc}(Q)$ is found by subtracting the counts from a 100% PSH blank to account for incoherent scattering and the counts from a 100% PSD blank to account for the total scattering ($S_T(Q)$). The correction law used is

$$I_{sc}(Q) = I_s(Q) - \left[\frac{a_H(1-x) + a_D x}{a_D} \right]^2 I_{s^{x=1}}(Q) - (1-x) I_{s^{x=0}}(Q) \quad (4)$$

All intensities are equal to the scattering cross sections multiplied by a single machine constant.

Results and Discussion

The samples measured are listed in Table I. These include samples with nearly matched and widely mismatched molecular weights and with high and low deuterated concentrations. We have elected to use the high-concentration matched samples as the standard against which to compare all other data. We have further elected to fit the data to a Debye function⁸ to determine the apparent R_g , assuming the chains in the bulk are ideal.⁹

Table III
 $\langle R_g^2 \rangle_w^{1/2}$ for Matched Molecular Weights

M_w	$\langle R_g^2 \rangle_w^{1/2} \pm 10\%, \text{ Å}$
194 000	119.8
93 500	83.6
58 000	62.3

Table IV
 $\langle R_g^2 \rangle_w^{1/2}$ for Mismatched Molecular Weights

M_w^D / M_w^H ^a	M_w	C_D / C_H ^b	measd $\langle R_g^2 \rangle_w^{1/2} \pm 10\%, \text{ Å}$	calcd $\langle R_g^2 \rangle_w^{1/2}, \text{ Å}$ ^c
0.87	87 000	0.80	84.8	78.8
	100 000		83.3	84.4
1.19	64 000	1.16	68.1	67.5
	53 700		56.2	61.9
0.32	64 000	0.30	64.1	67.5
	198 000		109.1	118.8
1.94	194 000	1.92	122.4	117.6
	100 000		90.0	84.4
3.60	194 000	6.15	103.3	117.6
	53 700		41.8	61.9
9.80	194 000	19.1	78.5	117.6
	19 800		11.3	37.6

^a M_w^D / M_w^H is the ratio of molecular weights of PSD and PSH as reported by light scattering and membrane osmometry. ^b C_D / C_H is equal to the ratio M_w^D / M_w^H as determined by the least-squares fit to the present data. ^c $\langle R_g^2 \rangle_w^{1/2}$ is calculated according to eq 7 with the value of K set equal to the average coefficient found from Table III.

Assuming the polydispersity follows a Schulz distribution, the corrected Debye function to be fit is¹⁰

$$g(y) = \frac{2}{(1+u)y^2} [y - 1 + (1+ux)^{-1/u}] \quad (5a)$$

where

$$y = \langle R_g^2 \rangle_z Q^2 / (1 + 2u) \quad (5b)$$

$$u = M_w / M_n - 1 \quad (5c)$$

The value of $\langle R_g^2 \rangle_w$ is then obtained from the fitted $\langle R_g^2 \rangle_z$ by¹¹

$$\langle R_g^2 \rangle_w = \langle R_g^2 \rangle_z \frac{1+u}{1+2u} \quad (6)$$

Table III gives the values of $\langle R_g^2 \rangle_w^{1/2}$ for the three pairs of samples with nearly matched molecular weights given in Table I. The $\langle R_g^2 \rangle_w^{1/2}$ were obtained by assuming the chains to be identical and applying eq 3 with an average molecular weight. When such samples are treated as having identical chains, the value of R_g is an average one that should compare well with the values calculated for each species separately using eq 1. Two of the pairs of samples used for Table III are repeated in Table IV (the first two pairs tabulated) and bear out the comparison. Using the values of Table III and assuming

$$\langle R_g^2 \rangle_w^{1/2} = K M_w^{1/2} \quad (7)$$

we are led to an average value of $K = (0.267 \pm 0.015) \times 10^{-8}$. The numbers shown in Table III are 7–8% lower than those obtained by Zimm plots as reported in a previous paper.³ This discrepancy we attribute to curvature in the Zimm plot until points are reached below $R_g Q = 1.0$. The data here reported do not extend to sufficiently low Q for accurate Zimm plot determinations.

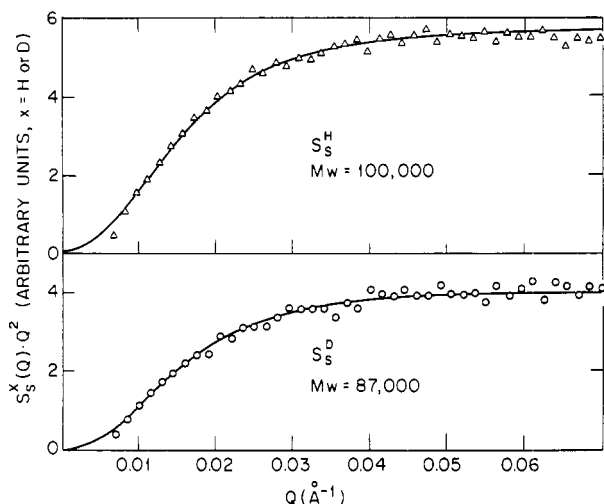


Figure 2. Kratky plots of $Q^2 S_s^H(Q)$ (Δ) and $Q^2 S_s^D(Q)$ (\circ) vs. Q obtained from the matched samples MPSH703 ($x = 0.3$) and MPSH3D7 ($x = 0.7$).

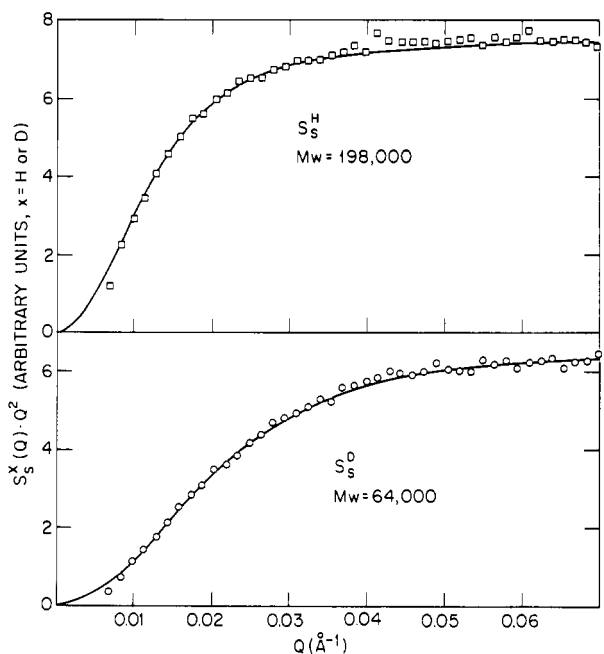


Figure 3. Kratky plots of $Q^2 S_s^H(Q)$ (\square) and $Q^2 S_s^D(Q)$ (\circ) obtained from the mismatched samples PSHH3LD7 and PSHH7LD3.

For samples with mismatched molecular weights the values of $(\langle R_g^2 \rangle_w^{1/2})^D$ and $(\langle R_g^2 \rangle_w^{1/2})^H$ are given in Table IV. For comparison of results using eq 1 and 3 the first two pairs of entries are two of the pairs treated as matched and reported in Table III. The calculated $\langle R_g^2 \rangle_w^{1/2}$ are the expected values using eq 7 and the coefficient K given above. The measured $\langle R_g^2 \rangle_w^{1/2}$ were obtained by solving eq 1 simultaneously for pairs of samples with different observed intensities and concentrations to extract $S_s^H(Q)$ and $S_s^D(Q)$. Each of these is then equated to the Debye function, eq 5, times an arbitrary constant, C . A least-squares fit is made with $\langle R_g^2 \rangle_w$ and the constant as fitting parameters. Finally, $\langle R_g^2 \rangle_w$ is obtained from eq 6. Since for any pair of samples C is actually a fixed constant times n_H or n_D , the ratio of fitted constants should agree closely with the known ratio M_w^D/M_w^H . These are compared in Table IV. Figure 2 gives Kratky plots for the measured values of $Q^2 S_s^H(Q)$ and $Q^2 S_s^D(Q)$ for the matched pair with $M_w^D/M_w^H = 0.87$. The solid curves are the fitted Debye functions. Figure 3 gives the same results for the mismatched pair with $M_w^D/M_w^H = 0.32$. The Kratky plots

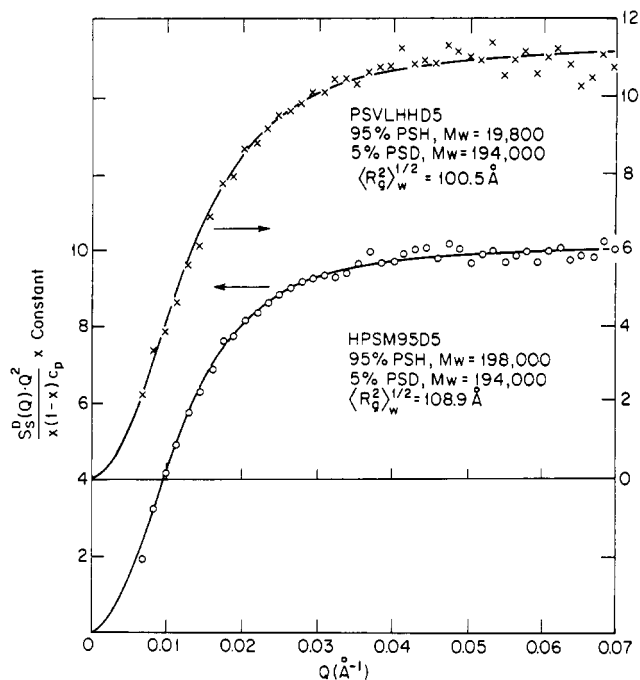


Figure 4. Kratky plots for 5% deuterated concentration samples, M_w of PSD = 198 000. The mismatched sample (\times) is PSVLHHD5 with 95% PSH, $M_w = 19 800$, and the matched sample (\circ) is HPSH95D5 with 95% PSH, $M_w = 194 000$.

for ratios of molecular weights greater than 3.0 are considerably poorer.

It is evident from Table IV that the radii of gyration, as measured and calculated by eq 1, compare well with values expected from samples with molecular weights assumed to be identical for mismatched weight ratios between 0.32 and 1.94. For the two cases of ratios 3.60 and 9.80 the comparison is progressively poorer. The same statements apply to the ratio M_w^D/M_w^H as determined by the fitting constants C_D/C_H when compared to the same ratio reported from light scattering and membrane osmometry.

We have attempted to verify the high-concentration numbers by performing some conventional low-concentration measurements. The characteristics of samples containing 5% deuterated molecules for both matched and highly mismatched molecular weights are included in Table I. The concentration of deuterated chains is 0.057 g/cm³ for both samples. This is smaller than the crossover concentration defined by

$$c^* = M_w / A \langle R_g \rangle_w^3 \quad (8)$$

where A is Avogadro's number. If K is defined as the number of statistical units per chain, then even for the highly mismatched sample $K_H > K_D^{1/2}$. Thus we expect to obtain equal values of $\langle R_g^2 \rangle_w^{1/2}$ for the two samples as well as agreement with the high-concentration results.¹² The Kratky plots for both samples are given in Figure 4 and the fitted values of $\langle R_g^2 \rangle_w^{1/2}$ are 108.9 Å for the matched sample HPSH95D5 and 100.5 Å for the mismatched sample PSVLH95D5. A second measurement on a separate pair of 5% samples yielded values of 111.4 and 101.8 Å. The averages for the two runs are thus 110.2 Å for the matched case and 101.2 Å for the mismatched case. These are 8% and 16%, respectively, below the expected value given in Table III. The disparity is just within experimental error for the matched sample but not for the mismatched case. Wignall et al.⁴ have shown, for matched molecular weight specimens, that the high-concentration

techniques give good consistency for concentrations down to 5%.

Conclusions

From the data of Table IV we conclude that eq 1 can be used to describe specimens for which the ratio $M_w(\text{PSD})/M_w(\text{PSH})$ lies between 0.32 and 1.94. The expression cannot be used for larger differences in the physical properties of the marked and unmarked molecules. This is demonstrated by the rapid deterioration of $\langle R_g^2 \rangle_w^{1/2}$ shown in Table IV for ratios of $M_w(\text{PSD})/M_w(\text{PSH})$ greater than 2.0. The derivation of eq 1 is based on a minimal dependence on x in the various scattering functions (eq 2a-c) and an agreement at a mismatch level as large as 3.0 is perhaps surprising.

Since eq 1 fails for large weight differences, the examination of such systems must, for the present, be studied by conventional low-concentration measurements. Our attempt to do so shows a significantly lower $\langle R_g^2 \rangle_w^{1/2}$ than should be expected on any physical grounds. It is possible that the concentration used was too high to ignore interference between marked chains.

The fact that for both low- and high-concentration samples the $\langle R_g^2 \rangle_w^{1/2}$ s obtained for large mismatch, for example, $n_D > 9n_H$, are very much lower than expected for matched molecular weights cannot be explained on any physical basis known to us. A change in the behavior of a long chain in the presence of smaller chains was earlier reported by Kirste for poly(dimethylsiloxane)¹³ but the change in $\langle R_g^2 \rangle_w^{1/2}$ is in a direction opposite to the present

data. There is evident need to explore such systems further.

Acknowledgment. We are grateful to D. F. R. Mildner and O. A. Pringle for their assistance on the MURR-SANS spectrometer.

References and Notes

- (1) Williams, C. E.; Nierlich, M.; Cotton, J. P.; Jannink, G.; Boue, F.; Daoud, M.; Farnoux, B.; Picot, C.; de Gennes, P. G.; Ri-
naudo, M.; Moan, M.; Wolff, C. *J. Polym. Sci., Polym. Lett. Ed.* **1979**, *17*, 379.
- (2) Ackasu, A. Z.; Summerfield, G. C.; Jahshan, S. N.; Han, C. C.; Kim, C. Y.; Yu, H. *J. Polym. Sci., Polym. Phys. Ed.* **1980**, *18*, 863.
- (3) Tangari, C.; Summerfield, G. C.; King, J. S.; Berliner, R.; Mildner, D. F. R. *Macromolecules* **1980**, *13*, 1546.
- (4) Wignall, G. D.; Hendricks, R. W.; Koehler, W. C.; Lin, J. S.; Wai, M. P.; Thomas, E. L.; Stein, R. S. *Polymer* **1981**, *22*, 886.
- (5) Summerfield, G. C. *J. Polym. Sci., Polym. Phys. Ed.* **1981**, *19*, 1011.
- (6) The PSH material and the PSD material with $M_w = 87\,000$ were supplied by Pressure Chemical Co. through L. Rosen. The PSD materials with $M_w = 64\,000$ and $M_w = 194\,000$ were prepared and characterized by Dr. L. Fetters, The University of Akron.
- (7) Mildner, D. F. R.; Berliner, R.; Pringle, O. A.; King, J. S. *J. Appl. Crystallogr.*, in press.
- (8) Debye, P. *J. Phys. Colloid Chem.* **1947**, *51*, 18.
- (9) Flory, P. J. *J. Chem. Phys.* **1949**, *17*, 303.
- (10) Greschner, G. S. *Makromol. Chem.* **1973**, *170*, 203.
- (11) Altgelt, K.; Schulz, G. V. *Makromol. Chem.* **1960**, *36*, 209.
- (12) de Gennes, P. G. "Scaling Concepts in Polymer Physics"; Cornell University Press: Ithaca, N.Y., 1979.
- (13) Kirste, R. G.; Lehnen, B. R. *Makromol. Chem.* **1976**, *177*, 1137.

Small-Angle X-ray Scattering Study of Perfluorinated Ionomer Membranes. 2. Models for Ionic Scattering Maximum

Mineo Fujimura, Takeji Hashimoto,* and Hiromichi Kawai

Department of Polymer Chemistry, Faculty of Engineering, Kyoto University, Kyoto 606, Japan. Received April 23, 1981

ABSTRACT: The origin of the "ionic scattering maximum", attributed to the presence of ionic clusters in perfluorinated ionomer membranes, was studied by computer simulations of the observed scattering profiles and of their variations with swelling and deformation of the membranes on the basis of two models: (i) the two-phase model, in which the ionic clusters (ion-rich regions) are dispersed in the matrix of the intermediate ionic phase composed of fluorocarbon chains and nonclustered ions (single ions, small multiplets), and (ii) the core-shell model, in which the ionic cluster (i.e., ion-rich core) is surrounded by the fluorocarbon phase (i.e., ion-poor shell), the core-shell particle itself being dispersed in the matrix of the intermediate ionic phase. A clear distinction between the models turns out to be generally difficult. That is, the general aspects of the variation of the scattering profiles with swelling and deformation can be described in terms of either of the two models, and thus the distinction between the models requires quantitative investigations of the scattering profiles in terms of shifts of the peak position and height and so on. However, the swelling behavior, especially the result that the microscopic degree of swelling as determined by small-angle X-ray scattering is much larger than the macroscopic degree of swelling, clearly supports the core-shell model, the "short-range order distance" of which gives rise to the ionic scattering maximum. The deformation behavior also tends to support the core-shell model, although it is less conclusive than the swelling behavior.

I. Introduction

In part 1¹ of this series we studied the small-angle X-ray scattering (SAXS) behavior of perfluorinated, carboxylated, or sulfonated ionomer membranes that were chemically modified from a series of Nafion² membranes having different equivalent weights (EW, i.e., the weight of polymer that will neutralize 1 equiv of base). We found two SAXS maxima: one at small s ($= (2 \sin \theta)/\lambda$, 2θ and λ being the scattering angle and the wavelength of the X-rays used in our experiments, 1.54 Å), which arises from

an interlamellar spacing, and the other at large s , which is designated as the "ionic scattering" maximum and which originates from the presence of ionic clusters, i.e., the region rich in ionic sites.

The size of the ionic clusters is experimentally found to depend on the kinds of cations and anions, the equivalent weight, the amount of water present in the membranes, and the temperature.¹ The dependencies of the cluster size on these physicochemical factors are shown to be predictable, at least in principle, in terms of the theory pro-